

Minivoids in the Local Volume

Anton V. Tikhonov

St. Petersburg State University, St. Petersburg, Russia

Igor D. Karachentsev

*Special Astrophysical Observatory, Russian Academy of Sciences, N. Arkhyz, KChR,
369167, Russia*

ABSTRACT

We consider a sphere of 7.5 Mpc radius, which contains 355 galaxies with accurately measured distances, to detect the nearest empty volumes. Using a simple void detection algorithm, we found six large (mini)voids in Aquila, Eridanus, Leo, Vela, Cepheus and Octans, each of more than 30 Mpc³. Besides them, 24 middle-size "bubbles" of more than 5 Mpc³ volume are detected, as well as 52 small "pores". The six largest minivoids occupy 58% of the considered volume. Addition of the bubbles and pores to them increases the total empty volume up to 75% and 81%, respectively. The detected local voids look like oblong potatoes with typical axial ratios $b/a = 0.75$ and $c/a = 0.62$ (in the triaxial ellipsoide approximation). Being arranged by the size of their volume, local voids follow power law of volumes-rankes dependence. A correlation Gamma-function of the Local Volume galaxies follows a power low with a formally calculated fractal dimension $D = 1.5$. We found that galaxies surrounding the local minivoids do not differ significantly from other nearby galaxies on their luminosity, but have appreciably higher hydrogen mass-to-luminosity ratio and also higher star formation rate. We recognize an effect of local expansion of typical minivoid to be $\Delta H/H_0 \sim (25 \pm 15)\%$

Subject headings: galaxies: general; cosmology: large-scale structure of Universe

1. Introduction

With the discovery of the first cosmic voids in the constellation Bootis (Kirshner et al., 1981) and in other sky regions (Joveer et al., 1978, Gregory and Tompson, 1978, de Lapparent et al., 1986, Rood, 1988), a new branch of extragalactic astronomy — "voidology" was formed. The concept of voids as basic elements of large-scale structure of the

Universe proved to be required in modern cosmological models. Zeldovich et al., 1982 considered giant volumes between superclusters which are almost empty of visible objects in the framework of structure formation theories. Ghigna et al. (1994) found that CDM models produce smaller void-probability function (VPF) than the observational one calculated on the volume-limited sub-sample of the Perseus-Pisces survey. Sheth and van de Weygaert (2004) presented a model for the distribution of void sizes and its evolution in the context of hierarchical scenarios of gravitational structure formation. Furlanetto and Piran (2005) produced a straightforward analytical model of the void distribution and of galaxy populations within voids. Patiri et al. (2005) compared statistical analysis of voids in 2dFGRS with that of cosmological N -body simulations and found that galaxies in voids are not randomly distributed but form structures like filaments. Icke (1984) on the basis of numerical studies concluded that voids between filaments are likely to be roughly spherical. Regoes and Geller (1991) found that in their models of structure formation in two and three dimensions, suitable initial conditions lead to cellular structure with faceted voids similar to those observed in redshift surveys. Icke and Van de Weygaert (1991), van de Weygaert (1994) introduced geometrical model - Voronoi foam (tessellations) for the skeleton of cosmic mass on scales 10 – 200 Mpc that includes voids as building blocks of large scale structure. Sahni et al. (1994) applied adhesion approximation to study the formation and evolution of voids in the universe. Peebles (2001) gave detailed review of modern status in theory and observations of voids.

Cosmic voids are usually considered to have typical dimensions of $\sim(20-50)$ Mpc, but the depth of voids, $\delta\rho / \langle \rho \rangle$, is the parameter which is still in question. Numerical modeling of the large-scale structure in Λ CDM models (Van de Weygaert and van Kampen, 1993, Gottlober et al., 2003, Sheth et al., 2004, Colberg et al., 2005) reproduces cosmic voids of different sizes and density contrast without conflicting with their typical observational parameters.

It is evident that the most reliable characteristics of voids can be obtained by investigating the nearest ones. In his Catalog and Atlas of Nearby Galaxies, Tully (1988) noted the presence in the Local Supercluster (LSC) of the so-called Local void which begins directly from the boundaries of the Local Group and extends in the direction of North Pole of the LSC by ~ 20 Mpc. The Local void looks practically free from galaxies. Karachentseva et al. (1998) undertook a search for new dwarf galaxies in the region of Tully void, but failed to find in it dwarf objects with luminosities down to 10^{-3} of the luminosity of the Milky Way. Recently Iwata et al. (2005) have measured velocities and distances of galaxies in a vicinity of the Local void and derived some evidence of its expansion. Studying the distribution of nearby galaxies in a volume of radius 10 Mpc, Karachentsev (1994) noted the presence in it of small voids of different sizes completely free from galaxies. As new galaxies were

discovered in this Local Volume and their individual distances were specified, the foamlike pattern structure of the Local Volume became more and more clear. This feature may prove to be universal, being a fractal continuation of the spectra of voids to small scales. At the present time, the sample of galaxies with distances less than 10 Mpc numbers about 450 galaxies. For half of them the distances have been measured to an accuracy as high as 8–10% (Karachentsev et al., 2004=CNG). The study of properties of voids in the most nearby sample, restricted by the distance, has an obvious advantage since we see here dwarf systems down to their minimum size/luminosity. This gives us unique possibility to define voids as regions empty of any type galaxies. According to scenarios of hierarchically evolving structure in the Universe voids are expected to contain some mass. But in this context our definition seems not to be unphysical because inside our voids we have certain amount of haloes of low masses that don't contain galaxies for different reasons. The absence of the effect of "God's fingers" in the Local Volume because of the virial motions of galaxies simplifies the analysis of the shape and orientation of nearby voids.

Below we undertake the first attempt to map voids in the Local Volume on the basis of quantitative reception of their finding. Here we present a list of nearby minivoids, maps of their distribution over the sky, and also discuss their shapes, orientations and characteristics of galaxies neighboring with voids.

2. The sample used for the void analysis

Until 2000, very little data had been available to describe the true 3D distribution of nearby galaxies even just around the Local Group. This surprising situation has been overcome recently with accurate distance measurements of nearby galaxies based on the luminosity of the tip of the red giant branch (TRGB). This method has a precision comparable to the Cepheid method, but requires much less observing time. Over the last five years, snapshot surveys with HST have provided us with the TRGB distances for many nearby galaxies obtained with an accuracy of 8 - 10%.

Apart from 36 members of the Local Group, there are so far 355 galaxies with distance estimates less than 7.5 Mpc. Among them, accurate distances to 183 galaxies have been measured based on the Cepheid method (N=12), or the luminosity of the TRGB (N=171). The remaining galaxies have only rough (25 - 30%) distance estimates from the luminosity of their brightest stars, the Tully-Fisher relation, or from their apparent membership to the known nearby groups. In this restricted distance range the TRGB method is most effective because it provides accurate distances to galaxies of all morphological types with minimal observational demands. A list of these galaxies is presented in "Catalog of Neighboring

Galaxies” by Karachentsev et al. (2004). The distribution of this galaxy sample over the sky is shown in Fig.1 by filled circles of different sizes according to distances of galaxies.

3. Void detection algorithm

There is no commonly accepted definition of void in galaxy distribution still. Different algorithms of void-finding give different list of voids. Some of them predefine shape of void (e.g. spherical), some search for volumes of arbitrary shape. It is worth to note the empty sphere method (Einasto, Einasto and Gramann, 1989), the variant with elliptical volumes (Ryden and Melott, 1996), the progressive construction of voids with cubes + rectangular prisms (Kaufmann and Fairall, 1991), the related method that uses connected spheres (El-Ad and Piran, 1997), the method of distance field maxima (Aikio and Mahonen, 1998), method of connected underdense grid-cells (Plionis and Basilakos, 2002), the use of the smoothed density field (Shandarin et al., 2006), the method of discrete stochastic geometry, namely, Delaunay and Voronoi tessellations (Schaap and van de Weygaert, 2000, Gaite, 2005). Grogin and Geller (1999, 2000) identified regions of low galaxy density by transformation of the point distribution of the CfA2 survey into continuously defined number density field in redshift space. We want to note also papers by Hoyle and Vogeley (2002, 2004) who determined voids in PSCz, UZC and 2dFGRS surveys by the voidfinder similar to (El-Ad and Piran, 1997) that divide galaxy population on void-galaxies and wall-galaxies with subsequent search for voids in distribution of wall-galaxies. Original approach made by Croton et al. (2004) - some scaling properties of 2dFGRS by the use of reduced VPF were revealed.

Nearly all of void-finders use some ad hoc parameter. For example in (El-Ad and Piran, 1997) it defines in what tunnel between galaxies void is allowed to penetrate and what tunnel is suppressed. Our method in some sense is close to (El-Ad and Piran, 1997). It is simple, flexible and appropriate for our definition of voids as regions completely free from galaxies.

In the volume of the sample under investigation an orthogonal three-dimensional lattice is constructed so that to refer the nodes of this grid to this or that void. The identification of voids is made from larger to smaller ones. First, a sphere with a largest radius of possible ones, which finds room inside empty (free from galaxies) regions of considered volume and geometric boundaries of the sample is detected. The voids are supposed to be exactly inside the geometric boundaries of the sample, therefore, the radius for a given node of the grid is determined as the smallest of distances: from the given node to nearest galaxy and a minimum distance from the node to boundary of the sample.

Inside the volume of the sample (Fig.2) a consecutive search for seed spheres (first the

largest sphere is sought for) free from galaxies executes with their subsequent expansion by means of addition of spheres whose centers are located inside the already fixed part of the void, and the radius R_{sph} is no less than that of the seed sphere multiplied by the coefficient $k = 0.9$ (i.e. $R_{sph} > 0.9 \cdot R_{seed}$, where R_{seed} is the radius of the seed sphere). Thus, the spheres added to the void intersect with the already referred to the void region by more than 30% of its volume. Further an empty sphere is identified again with the largest radius of possible with allowance made for the void identified at the previous step of void-finding (all the nodes of the grid referred to this void are excluded from the consideration), then it is expanded etc. Finding of voids continues until R_{seed} is larger than a certain specified threshold (in the present paper 0.5 Mpc).

When $k = 0.9$ the voids "represent" well enough the regions between galaxies and at the same time preserve a sufficiently regular form, which is convenient for subsequent approximation of voids by ellipsoids. At $k = 1$ voids will be strictly spherical. When diminishing k , the voids begin to penetrate into still smaller holes, and the shapes of voids become still more irregular. At small k one (first) void fills the greater part of the sample volume. The value of the coefficient $k = 0.9$ used in this paper is compromising, chosen after empirical detection of voids in distributions of points with different properties. The voids thus constructed (with $k = 0.9$) can be detected in volumes of arbitrary shape. On the other hand, the voids turn out to be separated from one another and "thick" enough throughout the entire their volume, which makes it possible to approximate them by triaxial ellipsoids.

The detected voids are divided into voids lying completely inside geometrical boundaries and into voids touching, when constructed, the sample boundaries, whose volumes are, consequently, underestimated, and the shapes are distorted by the boundary effect.

In the present paper the step of the lattice $Step = 0.1$ Mpc was used. The volumes of the voids were estimated as $Step^3 \cdot N$, where N is the number of nodes of the grid inside the given void. The described algorithm was applied to identification of voids between galaxies populating the Local Volume. Since with growing distance from the observer an abundance of galaxies of low luminosities drops, and the number of galaxies with accurately measured distances also decreases, we limited the search of voids with a sphere of radius 7.5 Mpc around us. This volume of 1766 Mpc³ contains 355 galaxies about 90% of which distance estimates measured irrespective of their radial velocities. Thus, the average volume for one galaxy is $V_1 = 5.0$ Mpc³ (the corresponding sphere radius is 1.06 Mpc).

The simulation of the procedure of voids detection at the Poisson distribution of galaxies with the same number density as in our sample has shown that voids with a volume of above 30 Mpc³ have sufficiently high statistical significance. There turned out to be six such voids in the volume considered. These minivooids are listed in the upper part of Table 1. Apart from

Table 1: Local minivoids and bubbles

Id	RA	DEC	D_c	R_{seed}	Volume	Constellation
	h	deg	Mpc	Mpc	Mpc ³	
1	19.02	2.9	3.80	3.33	443.6	Aquila
2	3.63	-12.6	4.40	2.94	159.8	Eridanus
3	9.52	22.8	3.92	2.38	219.5	Leo
4	8.51	-40.0	5.46	2.06	61.2	Vela
5	0.23	75.3	5.56	1.92	59.1	Cepheus
6	0.82	-86.0	5.39	1.86	85.2	Octans
7	23.77	-34.3	5.99	1.53	27.6	
8	13.70	30.0	6.09	1.43	19.8	
9	2.93	35.4	6.11	1.42	18.7	
10	0.77	22.3	6.20	1.31	18.5	
11	11.44	50.0	6.18	1.27	24.2	
12	12.28	-48.3	6.20	1.22	13.1	
13	15.50	60.6	6.36	1.16	13.6	
14	14.16	-31.5	6.38	1.14	12.8	
15	0.40	-8.1	6.37	1.13	9.3	
16	6.69	-6.8	6.39	1.12	9.6	
17	9.49	-9.5	6.40	1.12	14.3	
18i	10.96	-54.8	2.24	1.10	11.1	
19	5.18	19.6	6.41	1.09	11.7	
20i	8.34	85.0	2.19	0.99	11.1	
21	15.91	-52.5	6.50	0.99	12.9	
22	14.15	-0.8	6.55	0.95	8.4	
23	2.09	-47.5	6.54	0.94	5.0	
24	19.30	58.0	6.58	0.94	6.6	
25	5.64	-47.1	6.61	0.91	6.1	
27	23.27	41.4	6.62	0.90	5.4	
29	21.14	-55.8	6.58	0.89	8.4	
40	22.34	-22.9	6.72	0.70	7.0	
42	15.07	29.5	6.77	0.67	5.4	
43i	13.46	55.2	4.16	0.67	8.4	

them, our algorithm has found another 24 empty volumes whose sizes exceed the average volume V_1 . These "bubbles" are enumerated in the following 24 lines of Table 1. Finally, 52 smaller "pores" have been detected by the algorithm. The majority of them may be artefacts.

4. Census of the local minivoids and bubbles

The columns of Table 1 present the following data on 6 minivoids and 24 bubbles: (1) — ordinal number, (2,3) — equatorial coordinates of the center for the epoch J2000.0 in units of hours and degrees; (4) — distance to the center of the void in Mpc; (5) — radius of the seed sphere from which the building up of the empty volume takes place; (6) — volume of a minivoid or a bubble in Mpc^3 . It should be noted that the majority of empty volumes that we have discovered come in contact with the outer boundary of the sphere of radius 7.5 Mpc. Only 3 volumes out of 30 are fully inside into discussed sphere; they are marked by "i" at the ordinal number.

The distribution of the detected empty volumes over the sky in equatorial (a), galactic (b) and supergalactic (c) coordinates is shown in Fig.3. Six largest minivoids are presented by big circles, and 24 bubbles are depicted by small circles. All 355 galaxies of the Local Volume (filled circles) are broken up into three classes according to distances, where the blue color corresponds to the most nearby objects with $D < 2.5$ Mpc, the green color is for intermediate distances from 2.5 to 5.0 Mpc, while the red color corresponds to the most distant ones.

The fourth part of the whole Local Volume is occupied by void $N1$ in the constellation Aquilla. It represents the front part of the known Local void (Tully, 1988), which extends far beyond the limits of the volume under consideration. At the front boundary of this void a few dwarf galaxies (Sag DIG, DD0210, NGC6822) adjoining the Local group are located. As it follows from the distribution of voids in the galactic coordinates, only a minor part of them ($\sim 1/4$) can be due to the Galactic extinction.

The distribution over the sky of the 24 bubbles with respect to one another and to 6 largest minivoids does not show considerable association. Such an effect could be expected in the case where one or a few galaxies are situated inside a large void, breaking it up into two neighboring volumes.

We present in Fig.4 a 3D map which demonstrates the shape and mutual location of the 6 largest minivoids. To check an idea of the presence/absence in the empty volumes of dwarf

Table 2: Six the nearest bubbles/pores.

Id	RA	DEC	D_c	Volume	Neighboring galaxies
	h	deg	Mpc	Mpc ³	
72	7.53	-6.7	0.83	1.5	Phoenix, Fornax, LeoII, LMC
38	12.60	18.8	1.23	2.1	SexA, LeoI, LeoA, KK230
71	23.81	-48.8	1.32	1.1	WLM, Tucana, E294-010
20	8.34	85.0	2.19	11.1	M31, U8508, N1569, UA86, M82, KKH37
18	10.96	-54.8	2.24	11.1	N3109, E321-014, I3104, Circinus
26	0.54	-70.7	2.77	4.6	I3104, I5152

galaxies of extremely low luminosity or intergalactic hydrogen clouds of low ($M(HI) < 10^5 M_\odot$) masses, one can use data on six most nearby bubbles and pores (Table 2), the centers of which are within 3 Mpc from us. The designations of columns here are the same as in Table 1. The last column contains the names of galaxies located at the boundaries of these small voids. The 3D map of the distribution of the nearest bubbles/pores (Fig.5) shows tendency to locating their centers along the plane of the Local Supercluster.

5. Shape and orientation of the minivoids and bubbles

We approximate the surface of each empty volume identified by our algorithm by a equivalent triaxial ellipsoid that has the same moments of inertia as a body enclosed by the void. Their distribution with respect to the minor-to-major axial ratio, c/a , and the middle-to-major axial ratio, b/a , is shown in the upper panel of Fig.6. The ratios of axes for 30 minivoids and bubbles demonstrate a clear correlation characteristic of the prolate but not oblate configurations. The minor and major axes themselves are also correlated (lower panel of Fig.6), so that the mean ellipticity remains almost independent of the size of a void. Thus, the population of nearby voids looks like a set of oblong potatoes (or haricots), among

which there are no too flat or too long shapes. The distribution of the directions of the major axes of ellipsoids over the right half of the celestial hemisphere (Fig.7) does not show noticeable anisotropy. However, the spatial orientation of the major axes may take place in reality, with no evidence in projection on the sky.

6. Statistical properties of Local Volume

Being arranged by the size of their volume, local voids follow the Zipf power law $V(rank) \propto (rank)^{-z}$ with the exponent $z = 1.45$ (upper panel of Fig.8), which can be treated as a fractal character of distribution of voids (Gaité & Manrubia, 2002). Here, formally calculated fractal dimension is $D_z = 3/z \simeq 2.07$. However, one can not correctly measure a fractal dimension D of 3D fractal set based on the Zipf law unless $2 < D < 3$ since boundary of void has box dimension $D_b = 2$ (Gaité 2006). Application of our void-finder to different fractal sets showed this clearly. The value of D_z obtained by us is dangerously close to 2, therefore, we may put only an upper constraint, $D \leq 2.07$, on possible fractal dimension. We should note that we use here 'fractal' language as a simple approximation to the data and it will be interesting if other voidfinders would detect power law in the Local Volume since physical description in the frame of analytic model for the sizes of voids in galaxy distribution (Furlanetto and Piran, 2005) predicts a peaked void distribution. The total volume of the 6 minivoids is 58% of the volume considered. The addition of the 24 bubbles and 52 pores to them increases the total volume of voids up to 75% and 81%, respectively. The lower panel of Fig.7 shows a correlation Gamma-function (Coleman & Pietronero, 1992) of galaxies in the Local Volume. The variation of density with scale r in spheres, $\Gamma^*(r)$, and spherical shells, $\Gamma(r)$, follows a power law with an exponent $\gamma = 1.48$ (lower panel of Fig.8), which points to a formal fractal dimension $D_\Gamma = 3 - \gamma \simeq 1.5$ of the distribution of the Local Volume galaxies. A certain peculiarity in the Γ -function (bend) on a scale of ~ 3.5 Mpc may be associated with the characteristic distance between the centers of groups in the Local Volume. Simple fractal model of distribution of galaxies is not expected in modern scenarios of hierarchical structure formation and moreover it was rejected by statistical analysis (for example Tikhonov et al., 2000) and appears to be more complex - multifractal (Jones et al., 1992, McCauley, 2002, Jones et al., 2005). But nevertheless simple fractal dimension gives essential geometric description of distribution namely how galaxies fill given volume.

7. Galaxies around minivoids and bubbles

In different scenarios of formation of voids it is assumed (Peebles, 2001, Hoffman et al., 1992) that galaxies in voids may be different in their global parameters (luminosity, gas supply, star formation rate) from the population of denser regions, in particular, voids would be filled with galaxies of low luminosity. To check this assumption, we have considered in the Local Volume all galaxies which are located in layers 0.1 Mpc thick around empty volumes. The distribution of these galaxies according to their absolute blue magnitude M_B , hydrogen mass-to-luminosity ratio $M(HI)/L_B$ and star formation rate per unit luminosity $[SFR]/L_B$ in solar units are presented in three panels of Fig.9 (a, b, c, respectively). For comparison similar distributions of the whole sample of galaxies in the same volume are shown by opposite hatching. The data on hydrogen masses of galaxies have been taken from the catalog CNG, and the measurements of the star formation rate have been made from observations of the nearby galaxies in the H_α line (Karachentsev & Kaisin, 2006). As it follows from these diagrams, the expected differences of galaxies around the voids in the form of enhanced HI abundance and higher star formation rate (Peebles, 2001) do have actually take place. Their difference from the rest of galaxies manifests itself at a significance level $(2 - 3)\sigma$. In order to check the systematic differences of global properties of galaxies in dependence on their environment, we have applied a distinct approach similar to that of (Rojas et al., 2004). We have selected galaxies within a radius of 0.8 Mpc around of which no neighbors are present and compared them with the galaxies that have more than 5 neighbors within 0.3 Mpc. The distribution of these sub-samples in the parameters M_B , $M(HI)/L_B$, $[SFR]/L_B$ are displayed in Fig.10 a, b, c, respectively. The differences noted above for galaxies in loose and dense environment are seen here even clearer.

It should be emphasized that the assumption that the regions of low density are populated predominantly by objects of low luminosity is not confirmed by observations. The differences between galaxies around voids and in the general field are most likely of opposite character as to their luminosity (Fig.8a and 9a). The luminosity function of galaxies in dense environment looks wider since close interactions and mergers of galaxies leading to formation of faint “tidal” dwarfs and luminous mergers.

The galaxies surrounding nearby voids give us a unique opportunity to check whether the expansion of empty volumes does occur. In this case the galaxies located at the front boundary of a void will have radial velocities on average lower than in the homogeneous Hubble flow. On the farther side of a void the galaxies, correspondingly, have excess of radial velocities. We have selected on the near and back sides of the largest mini-voids 27 galaxies with accurately measured distances and velocities, and derived for them the mean difference of radial velocities $\langle \Delta V \rangle = (28 \pm 19) \text{ km s}^{-1}$. Here from the radial velocity of

each galaxy the regular Hubble component $V = H_0 D$ was subtracted with $H_0 = 72 \text{ km s}^{-1} \text{ Mpc}^{-1}$. Thus, on the scale of effective radius of typical local minivoid $\sim 1.5 \text{ Mpc}$ an effect of local expansion with an amplitude $\Delta H/H_0 \sim (25 \pm 15)\%$ is observed. The significance of the expected effect could be increased by means of measuring distances to other galaxies behind the nearby minivoids, which is quite possible now with the facilities of the Hubble Space Telescope.

8. Concluding remarks

When identifying voids in the Local Volume, we were based on the assumption that minivoids, bubbles and pores are completely free from galaxies. This assumption, important in theoretical models (Peebles, 2001), can be tested in subsequent observations. The "blind" survey of the whole southern sky made in the HI line of neutral hydrogen at the 64-m Parks radio telescope led to detection of new dwarf galaxies, in particular, in the Zone of Avoidance of the Milky Way (Kilborn et al., 2002, Staveley-Smith et al., 1998). A similar survey of the northern sky is conducted in Jodral Bank (Boyce et al., 2001). A much more sensitive blind survey in the HI line is now conducting at the 300-m radio telescope in Arecibo (Giovanelli et al., 2005). The minivoids Aquia, Leo, Eridanus as well as six other bubbles of smaller size fall partially within the zone of the Arecibo survey, $\text{DEC.} = [0, + 38^\circ]$. We expect that the results of this survey will have a chance to confirm or reject the idea of complete absence of galaxies in nearby voids. The detection of new nearby galaxies and measurement of their distances from the luminosity of red giant branch stars will allow a more detailed study of the shape and kinematics of the nearest voids. As was noted above, the Local void in Aquila, detected by Tully, extends far beyond the limits of the Local Volume. By the present time, the number of nearby galaxies with radial velocities $< 3000 \text{ km s}^{-1}$ has reached about seven thousand. This new observational material presents a possibility of detecting and investigating voids by two orders of magnitude exceeding the volume considered here.

The authors are grateful to S. Shandarin, D. Makarov, J. Gaite and B. Tully for useful advices and discussions. Support associated with HST programs 9771 and 10235 was provided by NASA through a grant from the Space Telescope Science Institute, which is operated by the Association of Universities for Research in Astronomy, Inc., under NASA contract NAS5-26555. This work was also supported by RFFI grant 04-02-16115 and by grant Rosobrazovanie RNP 2.1.1.2852.

REFERENCES

- Aikio J., Mahonen P., 1998, *ApJ*, 497, 534
- Boyce P.J., et al. 2001, *ApJ*, 560, L127
- Colberg J.M., Sheth R.K., Diaferio A. et al., 2005, *MNRAS*, 360, 216
- Coleman P.H., Pietronero L., *Physics Reports*, 1992, 213, 311
- Croton D., Colles M., Gaztanaga E. et al., 2004, *MNRAS*, 352, 828
- de Lapparent V., Geller M.J., Huchra J.P., 1986, *ApJ*, 302, L1
- Einasto J., Einasto M., Gramann M., 1989, *MNRAS*, 238, 155
- El-Ad H., Piran T., 1997, *ApJ*, 491, 421
- Furlanetto S. and Piran T., 2005,
- Gaite J., Manrubia S.C., 2002, *MNRAS*, 335, 977
- Gaite J., 2005, *Eur.Phys.J. B47*, 93, astro-ph/0506543
- Gaite J., 2006, preprint (astro-ph/0603572)
- Ghigna S., Borgani S., Bonometto S., et al. 1994, *ApJ*, 437, L71
- Giovanelli R., Haynes M., Karachentsev I. et al., 2005, *AJ*, 130, 2598
- Gottlober S., Lokas E., Klypin A., Hoffman Y., 2003, *MNRAS*, 344, 715
- Gregory S.A., Thompson L.A., 1978, *ApJ*, 222, 784
- Grogin and Geller, 1999, *AJ*, 118, 2561
- Grogin and Geller ,2000, *AJ*, 119, 32
- Hoffman Y., Silk J., Wyse R., 1992, *ApJ*, 388, 13
- Hoyle F. and Vogeley M., 2002, *ApJ*, 566, 641
- Hoyle F. and Vogeley M., 2004, *ApJ*, 607, 751
- Icke V., 1984, *MNRAS*, 206, Short Communication, 1P
- Icke V., Van de Weygaert R., 1991, *QJRAS*, 32, 85

- Iwata I., Ohta K., Nakanishi K., et al., 2004, in "Nearby Large-Scale Structures and the Zone of Avoidance", ASP Conference Series, v. 329, eds. A.P.Fairall, P.A.Woudt, p. 59
- Joeveer M., Einasto J., Tago E., 1978, MNRAS, 185, 357
- Jones B., Coles P., Martinez V., 1992, MNRAS, 259, 146
- Jones B., Martinez V., Saar E., Trimble V., 2005, Reviews of Modern Physics, 76, 1211
- Karachentsev I.D., 1994, Astron. & Astrophys. Trans. 6, 1
- Karachentsev I.D., Kaisin S.S., 2006, in preparation
- Karachentsev I.D., Karachentseva V.E., Huchtmeier W.K., Makarov D.I., 2004, AJ, 127, 2031 (=CNG)
- Karachentseva V.E., Karachentsev I.D., Richter G.M., 1998, A&A, 135, 221
- Kauffmann G., Fairall A.P., 1991, MNRAS, 248, 313
- Kilborn, V.A., Webster, R.L., Staveley-Smith, L. et al. 2002, AJ, 124, 690
- Kirshner R.P., Oemler A., Schechter P.L., Sackett P.A., 1981, ApJ, 248, L57
- McCauley J.L., Physica A, 2002, 309, 183, astro-ph/9703046
- Patiri S.G., Betancort-Rijo J., Prada F., et al., 2005, astro-ph/0506668
- Peebles P.J.E., 2001, ApJ, 557, 495
- Plionis M., Basilakos S., 2002, MNRAS, 330, 399
- Regoes E., Geller M., 1991, ApJ, 377, 14
- Rojas R., Vogeley M., Hoyle F., Brinkmann K., 2004, ApJ, 617, 50
- Rood H.J., Annual review of astronomy and astrophysics, 1988, 26, 245
- Ryden B.S., Melott A.L., 1996, ApJ, 470, 160
- Sahni V., Sathiaprakash B., Shandarin S., 1994, ApJ, 431, 20
- Schaap, van de Weygaert, 2000, A&A, 363, L29-L32
- Shandarin S., Feldman H.A., Heitmann K., Habib S., 2006, MNRAS, 367, 1629

Sheth R.K., Van de Weygaert R., 2004, MNRAS, 350, 517

Staveley-Smith, L., Juraszek, S., Koribalski, B.S. et al. 1998, AJ, 116, 2717

Tikhonov A.V., Makarov D.I., Kopylov A.I., 2000, Bull. SAO RAS, 50, 39, astro-ph/0106276

Tully R.B., 1988, Nearby Galaxy Catalog, Cambridge University Press

Van de Weygaert R., 1994, A&A, 283, 361

Van de Weygaert R., van Kampen E., 1993, MNRAS, 263, 481

Zeldovich, Ia. B., Einasto, J., Shandarin, S. F., 1982, Nature, 300, 407

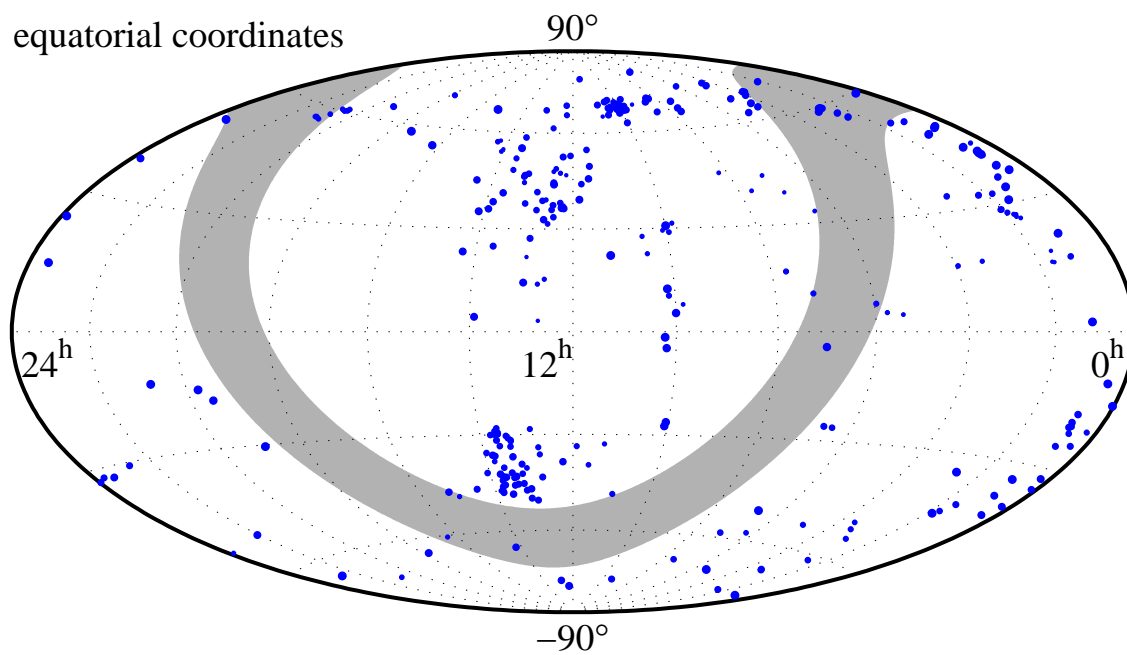


Fig. 1.— All-sky distribution of Local Volume galaxies with distances less than 7.5 Mpc in equatorial coordinates. Sizes of circles decrease in accordance with increasing of distances of galaxies. The shaded area marks the Zone of Avoidance in the Milky Way.

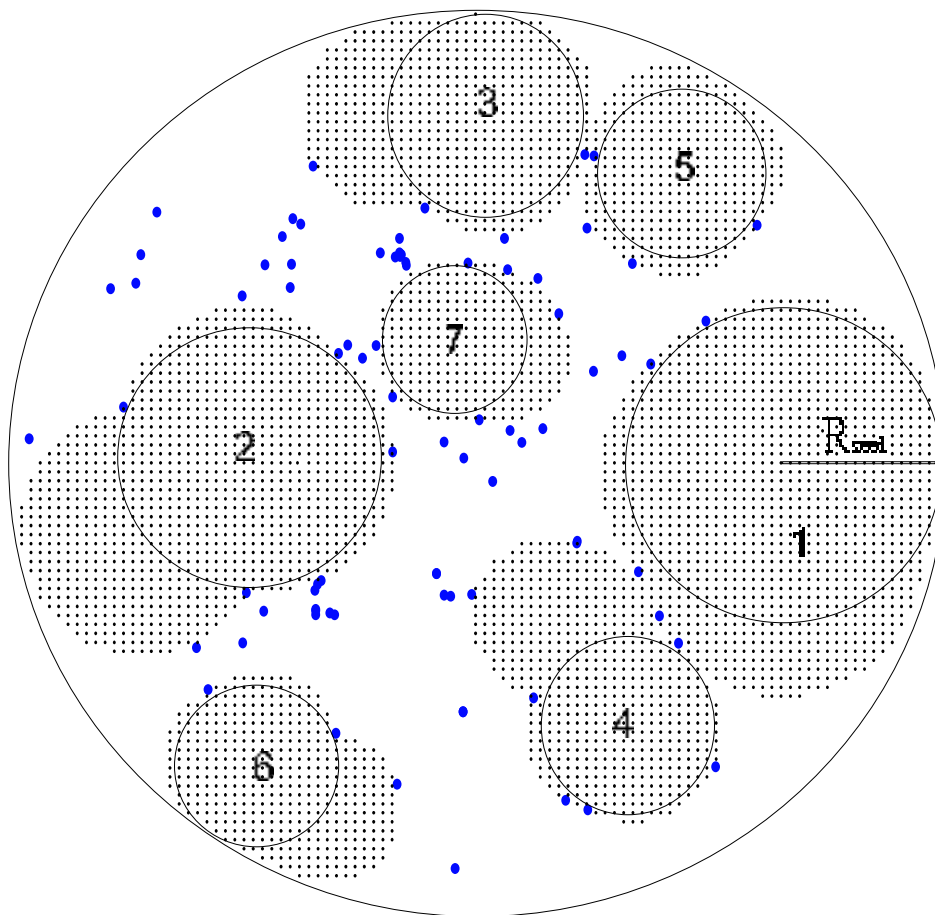


Fig. 2.— Illustration of action of the void-finding algorithm in a case of 2D point-like distribution. Seed spheres and voids growing from them are shown. The numerals indicate the order of detection of voids from large seed spheres to smaller ones.

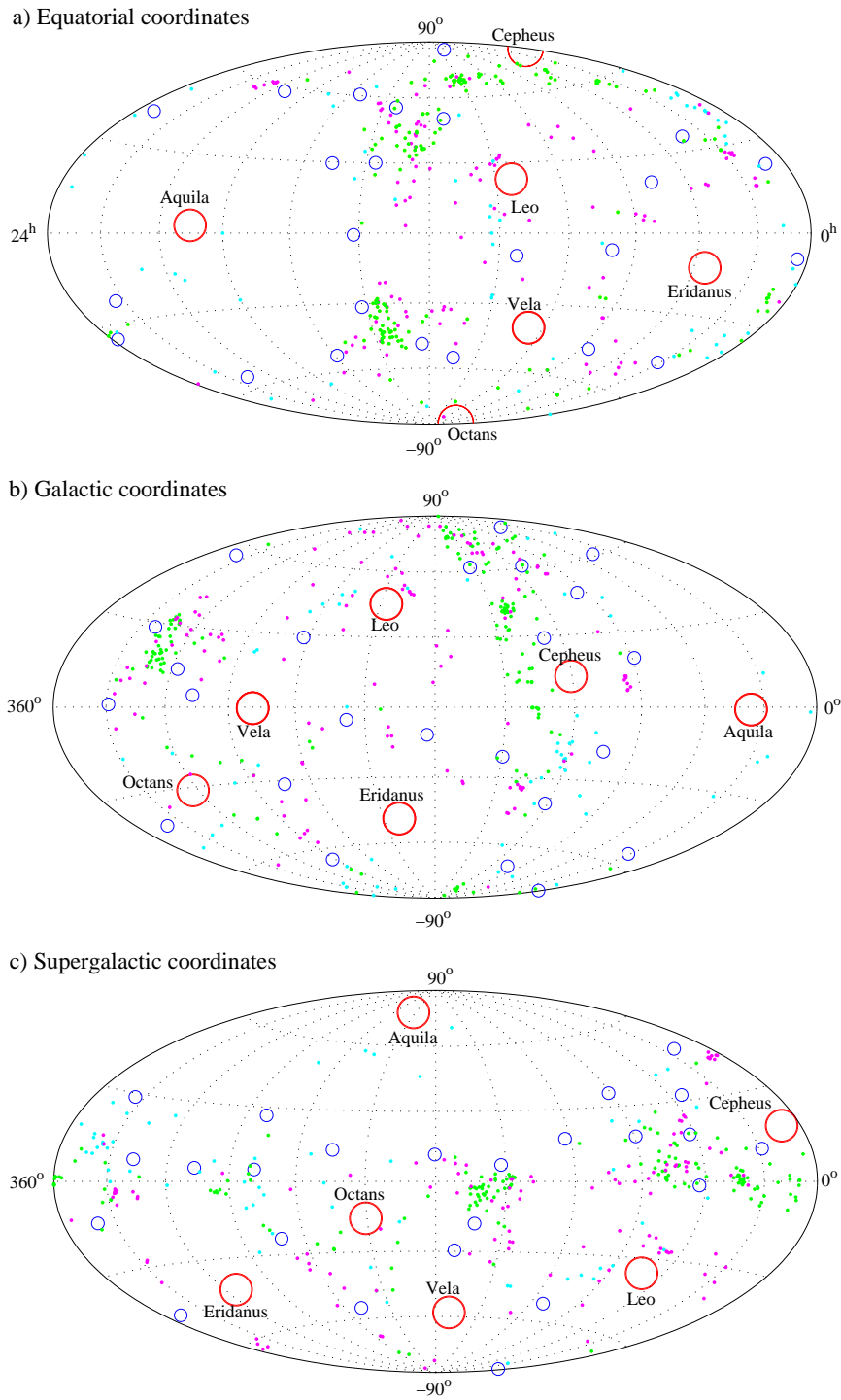


Fig. 3.— Distribution over the celestial sphere of six large minivoids (large red circles around void centers), 24 bubbles (small blue circles) and the Local Volume galaxies with distances $D < 2.5$ (blue), $2.5 < D < 5$ (green) and $5 < D < 7.5$ (red).



Fig. 4.— Distribution of six large minivoids within the sphere of radius 7.5 Mpc.



Fig. 5.— Distribution of two nearest bubbles (No 20 and 18) and four pores (No 72, 38, 71, 26) with distances to their centers less than 3 Mpc. Perspective is XZ plane in equatorial coordinates. The circle indicates the Milky Way location.

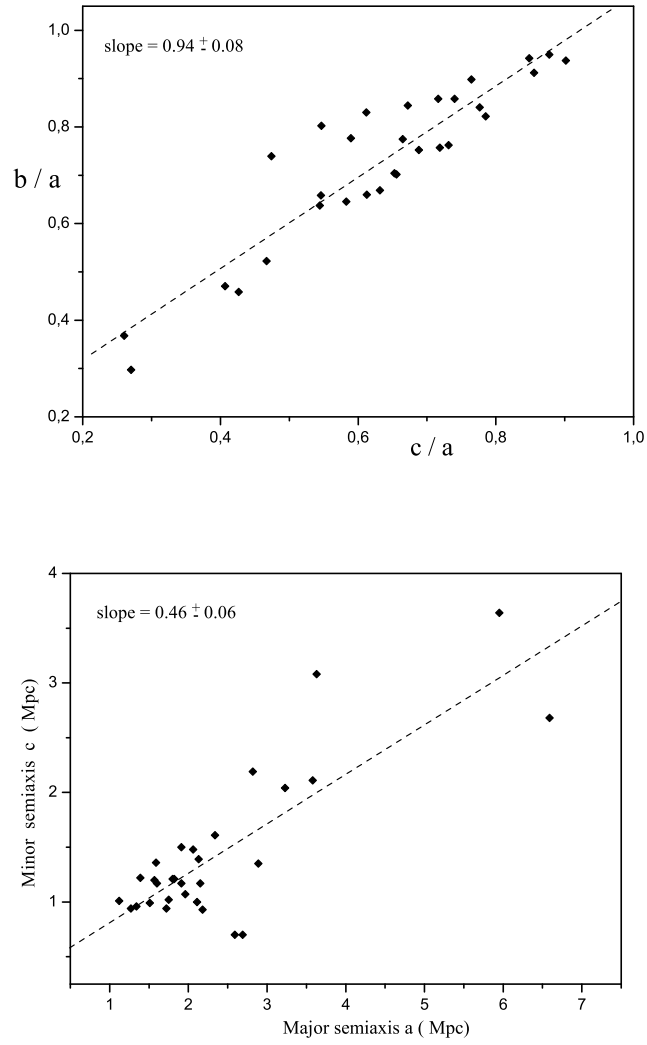


Fig. 6.— (Top) Relationship among axial ratios of 30 minivoids and bubbles: minor-to-major, c/a , and middle-to-major, b/a , axial ratios of equivalent ellipsoids. (Bottom) Relationship among the semi-major and semi-minor axes of equivalent ellipsoids for the same voids.

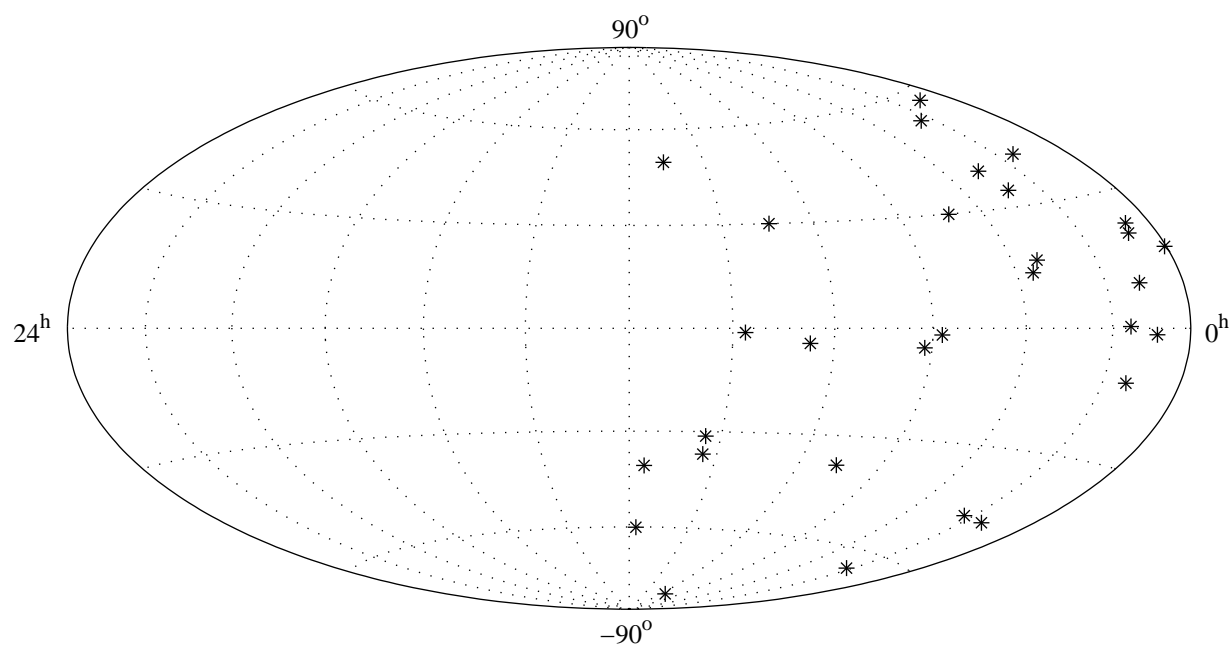


Fig. 7.— A view of directions of the major axes of 30 voids distributed over the right half of the celestial sphere.

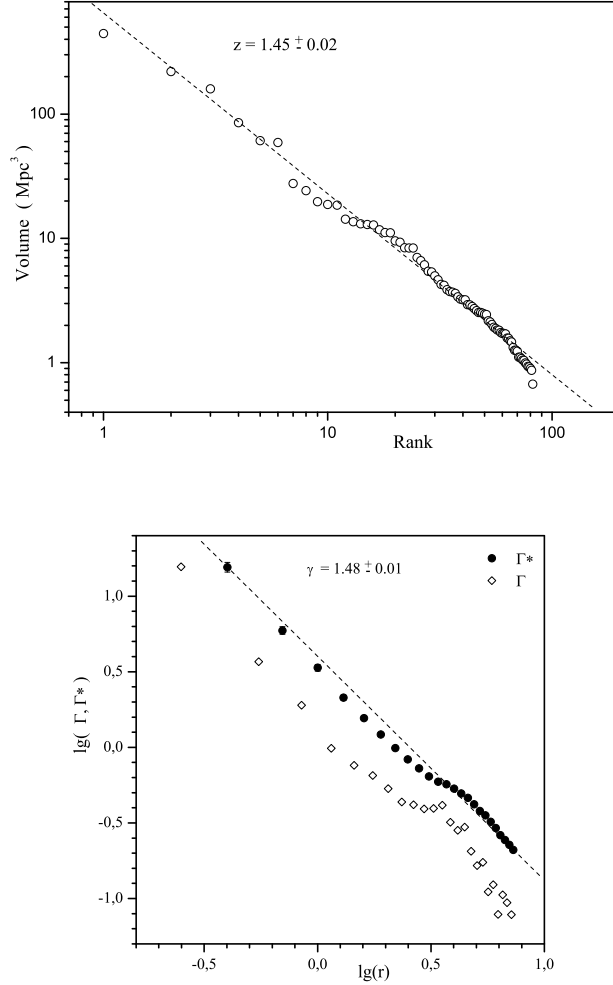


Fig. 8.— (Top) The void volumes versus their ranks in \log_{10} scale. Power law is evident. (Bottom) Correlation Gamma-function of 355 galaxies in Local Volume within a sphere of radius 7.5 Mpc.

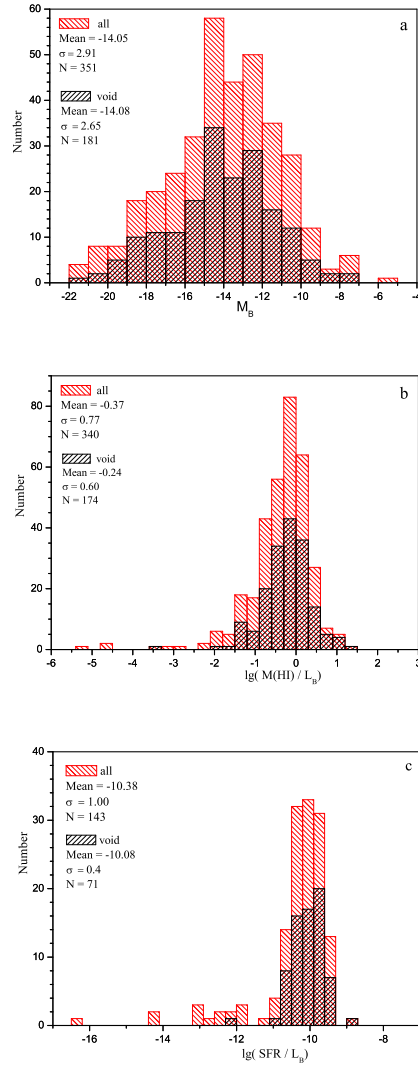


Fig. 9.— (a) - B-band absolute magnitude distribution of the Local Volume galaxies and galaxies around local voids; (b) - ratio of hydrogen mass to blue luminosity in solar units; (c) - star formation rate per unit of blue luminosity.

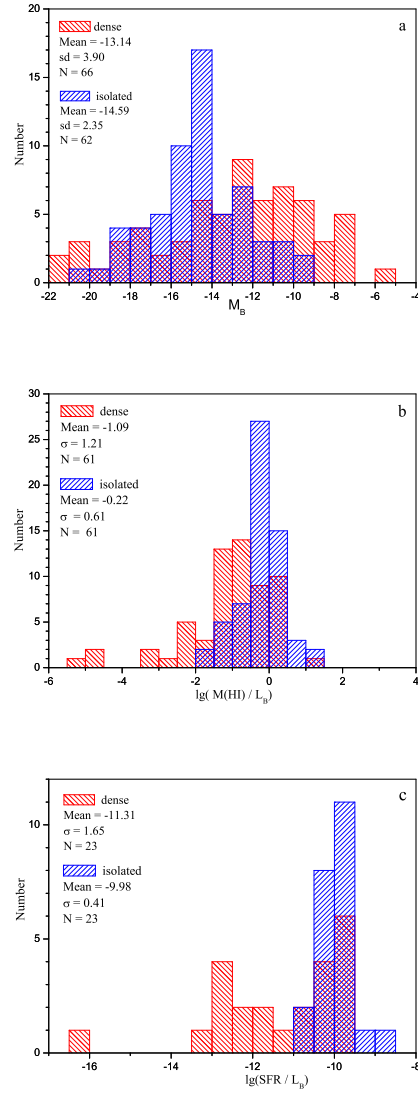


Fig. 10.— (a) - B-band absolute magnitude distribution of isolated galaxies and galaxies in dense environment of the Local Volume; (b) - ratio of hydrogen mass to blue luminosity in solar units; (c) - star formation rate per unit of blue luminosity.